

Enhancement of persistent current in a non-Hermitian disordered ring

Suparna Sarkar,^{1,*} Soumya Satpathi,^{1,*} and Swapan K. Pati^{1,†}

¹*Theoretical Sciences Unit, School of Advanced Materials (SAMat),
Jawaharlal Nehru Centre for Advanced Scientific Research, Bangalore 560064, India*

(Dated: February 19, 2025)

We have studied the Aharonov-Bohm flux-induced magnetic response of a disordered non-Hermitian ring. The disorder is introduced through an on-site quasiperiodic potential described by the Aubry-André-Harper (AAH) model, incorporating a complex phase that renders the model non-Hermitian. Our findings reveal that this form of non-Hermiticity enhances the persistent current, without requiring hopping dimerization. We explore both non-interacting and interacting scenarios. In the former, we examine spinless fermions, while in the latter, we consider fermions with Hubbard interactions. The Non-Hermitian phase induces both the real and imaginary components of the current. We thoroughly analyze the energy eigenspectrum, ground state energy, and persistent current in both real and imaginary spaces for various system parameters. Our primary goal is to investigate the combined effects of non-Hermiticity and disorder strength on persistent currents. We find an enhancement in both the real and imaginary components of the persistent current with increasing disorder strength, as well as the non-Hermiticity, up to a critical value. Furthermore, we observe an enhancement in persistent current in the presence of Hubbard correlation. Our findings may provide a new route to get nontrivial characteristics in persistent current for a special type of non-Hermitian systems.

I. INTRODUCTION

In the presence of a magnetic flux, a normal metal ring sustains a non-dissipative current at very low temperature. This is known as persistent current and it arises from the Aharonov-Bohm (AB) effect, where electron wave functions acquire a phase shift due to the enclosed magnetic flux. It was initially proposed by Büttiker et al. in 1983 [1] and later the first experimental confirmation came in 1990 when Lévy et al. [3] observed persistent currents in small metallic rings. After that, the concept of persistent currents has inspired extensive exploration, both theoretically [4–9] and experimentally [10–13], across a large variety of quantum systems. Since the response of PC with magnetic flux is very sensitive to disorder, a large number of studies have already explored PC in uncorrelated as well as correlated disordered rings [14–16]. Among various correlated systems, one of the most well-known and remarkable ones is the Aubry-André-Harper (AAH) model [19–22]. It is quite obvious that the average persistent current (PC) amplitude decreases with increasing disorder [17, 18]. Interestingly, recent studies have revealed that along with AAH disorder within Su-Schrieffer-Heeger (SSH) rings [23] an enhancement in the amplitude of persistent currents can be obtained, suggesting that the interplay between hopping dimerization and quasiperiodic disorder can counteract disorder-induced suppression.

In the studies mentioned above, all theoretical investigations are based on Hermitian models. However, very recently, the interplay between disorder and non-Hermiticity in systems governed by non-Hermitian Hamiltonians has attracted considerable attention [24–29]. Non-Hermitian systems are becoming popular for

the wide array of intriguing physical phenomena that remain unattainable in their Hermitian counterparts. In particular, systems exhibiting parity-time (PT) symmetry have attracted significant interest. This symmetry ensures a completely real energy spectrum below a critical threshold [30–32]. Recently PC has been explored in a dimerized non-Hermitian ring [33–35] where the non-Hermitian effects have been introduced either from non-reciprocal hopping terms or by physical gain and loss at different sites.

The information above has led us to find any other alternative non-Hermitian Hamiltonian in which we can get an enhanced persistent current without considering dimerized hopping. To do this, we have introduced diagonal AAH disorder with complex phase factor in a one-dimensional mesoscopic ring and for the first time we have explored the characteristics of persistent current by considering this form of non-Hermiticity. Furthermore, the impact of non-Hermitian effects on persistent currents in interacting systems with nonzero electron-electron correlations remains completely unexplored in the literature. Previous studies for Hermitian systems have shown that moderate interactions can enhance persistent currents in half-filled or partially filled ring systems, particularly in the presence of weak disorder [36, 37]. While electron-electron interactions have been extensively studied in Hermitian systems, the effects of non-Hermitian quasi-periodicity in interacting systems remain largely unexplored. This gap in the literature presents an exciting opportunity for further investigation, as the interplay between non-Hermitian effects, quasi-periodicity, and electron-electron interactions may lead to novel phenomena and rich physical insights, in the context of quantum transport and persistent current.

Describing the system within a tight-binding framework, we calculate persistent current from ground state energy by differentiating with respect to the magnetic flux and study the interplay between disorder strength and non-Hermiticity. In the present work, we address the

* These authors contributed equally to this work.

† pati@jncasr.ac.in

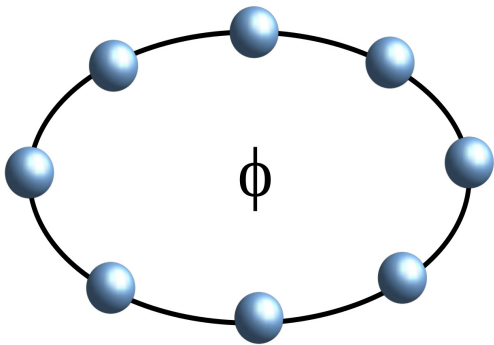


FIG. 1. (Color online) Schematic diagram of an isolated one dimensional ring threaded by a AB flux.

following important issues: (i) The variation of ground state energy and persistent current with phase for different values of the strength of non-Hermiticity shows an enhancement of the real and imaginary parts of PC with non-Hermiticity, (iii) Up to a certain threshold value, both the real and imaginary currents increase with disorder strength, (iv) For the interacting scenario for finite size ring, we obtain more current for higher disorder value, (v) an enhancement of persistent current occurs with Hubbard correlation up a certain critical value.

The structure of the remaining sections is as follows: In Section II, we describe the model, the TB Hamiltonian, the many-body Hamiltonian and the theoretical approach used to obtain the results. Sec. III presents all the results in an organized manner and examines them thoroughly. Finally, we conclude our work in Section IV.

II. MODEL AND METHODS

As illustrated in Fig. 1, we consider a non-Hermitian Aubry-André-Harper (AAH) quasiperiodic ring characterized by complex potentials subjected to an AB flux. The tight-binding Hamiltonian of the ring for spinless interacting fermions can be written as

$$H = t \sum_{i=1}^L e^{-iqA} (c_{i+1}^\dagger c_i + h.c.) + \sum_{i=1}^L \epsilon_i n_i, \quad (1)$$

where L represents the total number of sites in the lattice. The operators $c_i^\dagger (c_i)$ correspond to the fermionic creation (annihilation) operator at site i , while $n_i = c_i^\dagger c_i$ denotes the fermion number at that site. The AAH model is characterized by the functional form $\epsilon_i = W_i \cos(2\pi b i + \phi_\nu)$, where W determines the strength of the cosine modulation at each site. The parameter b is an irrational number ($b = (\sqrt{5} - 1)/2$), introducing an aperiodic nature to the lattice. Here, A represents the magnetic vector potential. The phase factor ϕ_ν , which is linked to the AAH modulation, plays a crucial role as it can be externally adjusted through an appropriate experimental setup [34]. In this context, we set $\phi_\nu = j\hbar$, here j corresponds to $\sqrt{-1}$ and the complex phase, h controls the degree of non-Hermiticity within the system.

In a spinless system, following the Pauli exclusion principle, electrons sequentially occupy energy levels starting from the lowest available level at absolute zero temperature. The ground state energy of the system is determined by summing the energies of all occupied levels up to where corresponds to the highest occupied energy level for a given number of electrons,

$$E_0^{re/im} = \sum_m^{Ne} E_m^{re/im} \quad (2)$$

at zero temperature where $E_0^{re/im}$ denotes the ground state energy and E_m is the eigenvalue of m th state. Since this is a non-Hermitian (NH) system, we observe both real and imaginary eigenvalues, necessitating the calculation of E_0 in both the real and imaginary domains. Hence, to compute the current in this case, we employ the following definition [33, 34]:

$$I^{re/im} = -c \frac{\partial E_0^{re/im}}{\partial \phi} \quad (3)$$

where c is a constant.

For interacting case, we consider a interacting fermions with spin, and incorporate electron-electron interactions via an on-site interaction Hubbard term, U in the Hamiltonian. The total Hamiltonian is expressed as

$$H = H_0 + H_U \quad (4)$$

where H_0 represents the non-interacting part of electrons with spin degrees of freedom together with incorporating the effects of AAH modulation and non-Hermiticity, while H_U accounts for the on-site electron-electron interactions introduced by the Hubbard term;

$$H_0 = t \sum_{i=1}^L \sum_{\sigma} e^{-iqA} (c_{i+1}^\dagger c_i + H.c.) + \sum_{i=1}^L \sum_{\sigma} \epsilon_i n_{i,\sigma} \quad (5)$$

In the numerical calculations, t will be set to 1, and ϵ_i is modulated as mentioned above and

$$H_U = U \sum_{i=1}^L n_{i,\uparrow} n_{i,\downarrow} \quad (6)$$

accounts for the electronic interactions. For numerical analysis, energy spectra are computed using exact diagonalization for system sizes up to 12 sites.

III. NUMERICAL RESULTS AND DISCUSSION

In this section, we present our numerical results for the non-interacting case and explore the influence of non-Hermiticity on the persistent current within our system. Our analysis is conducted at half-filling, offering an ideal framework for examining the system's behavior. All hopping integrals and energy eigenvalues are expressed in electron volts (eV), while the current is measured in microamperes (μA).

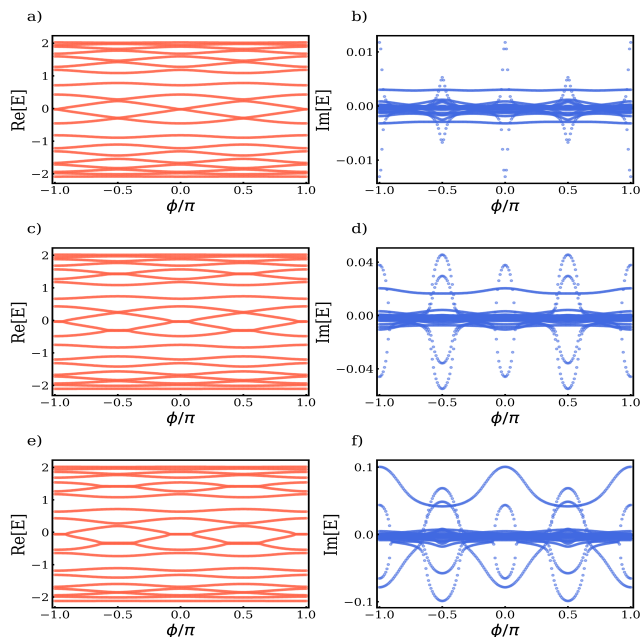


FIG. 2. (Color online) Variation of real and imaginary energy eigenspectra as a function of AB flux where the first, second, and third rows are for $h = 0.25, 0.75,$ and 1 respectively.

A. Energy Spectrum and Current varying h

The energy spectrum is illustrated as a function of flux in Fig. 2. The left column exhibits spectra characterized by real eigenvalues, while the right column showcases those distinguished by imaginary eigenvalues. The imaginary and real parts of the eigenvalues are represented by the royal blue and tomato-colored spectra, respectively; for various values of the complex phase, $h(0.25, 0.75, 1.0)$ (upper, middle, and lower row respectively). The energy levels in the real spectrum have finite slopes and substantial degeneracy; some of these slopes get canceled with each others out. As the strength of the complex phase increases, the degeneracy of certain energy levels is lifted, and fewer slopes cancel each other out, potentially enhancing the persistent current. In the imaginary part of the eigenvalues, we observe that at $h = 0.25$, most of the energy levels cluster around zero, forming a highly degenerate band. However, as the strength of the complex phase increases, additional energy bands begin to emerge. Moreover, there exist certain distinct points where the energy levels diverge, commonly referred to as the exceptional points.

With the energy spectrum established as a function of flux(ϕ), we can now investigate the behavior of the PC. We examine how the ground state energy changes with magnetic flux, considering both its real and imaginary parts, since the slope of the ground state energy is what essentially determines the PC. In Fig. 3, we present a comparative visualization by plotting the ground state energy alongside the corresponding current for a clearer understanding. The upper row illustrates the real part of the eigenvalues and the associated current, while the lower row displays the imaginary part of the eigenvalues

and its corresponding current, for various values of h .

Both the real and imaginary parts of the ground state energy vary continuously with flux. However, at specific exceptional points, the slope changes abruptly, causing sharp spikes in the current. As the strength of the complex phase, h increases, these slope variations become more significant, leading to an enhanced persistent current with increasing h .

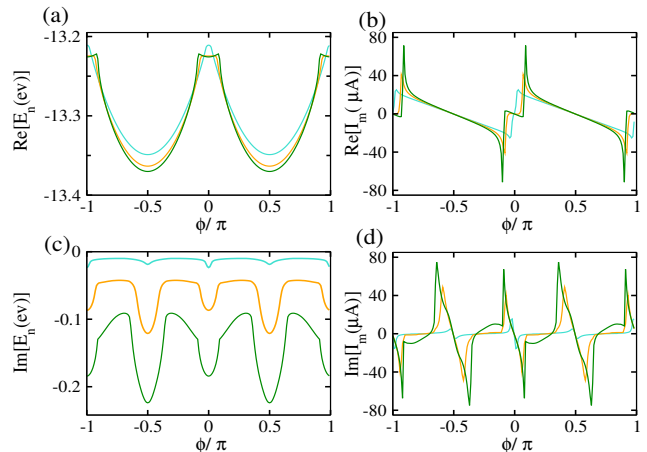


FIG. 3. (Color online). Real and imaginary parts of the ground state energy versus AB flux ((a) and (c)) and that of maximum PC versus AB flux ((b) and (d)) where cyan, orange and green curves represents the results for $h = 0.25, 0.75$ and 1 respectively.

B. Energy Spectrum and Current varying W

We have also plotted the energy spectrum as a function of the AAH strength while keeping the complex phase fixed at $h = 1.0$. In Fig. 4, the left column shows spectra with real eigenvalues, while the right column shows those with imaginary eigenvalues for different values of AAH strength ($W = 0.25, 0.5, 0.75$) (upper, middle, and lower row respectively). Similar to previous observations in the real part of the eigenvalues; increasing the strength of W lifts the degeneracy of certain energy levels which in effect reduces the number of slope cancellations. This effect can potentially enhance the PC by allowing more energy levels to contribute constructively to the current flow.

In the imaginary part of the eigenvalues, we observe that at $W = 0.25$, most energy levels cluster around zero, forming a highly degenerate band, except at a few exceptional points where certain energy levels spread out. As W increases to 0.5 , additional energy bands emerge, contributing to a rise in the persistent current. However, at a higher $W = 1$, the spectrum develops a gapped spectrum with three distinct sub-bands. In the band near the middle of the spectrum, most slopes cancel each others out, leading to a reduction in the persistent current compared to the $W = 0.5$ case.

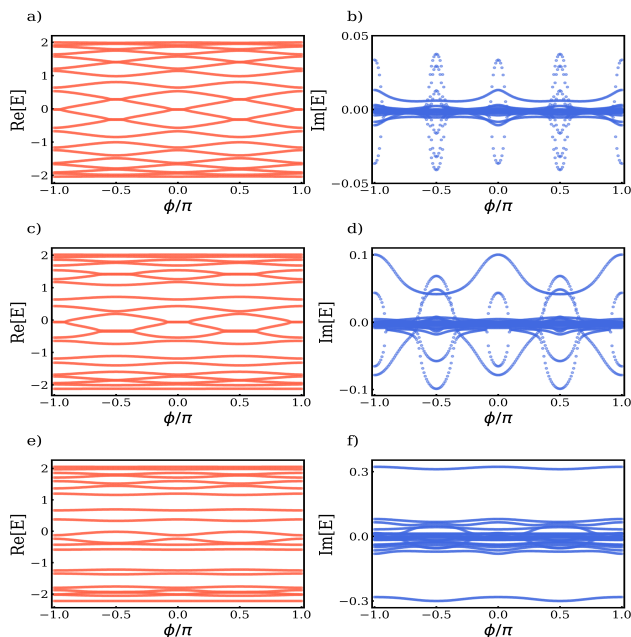


FIG. 4. (Color online). Variation of real and imaginary energy eigenspectra as a function of AB flux where the first, second, and third rows are for $W = 0.25, 0.5$ and 0.75 respectively.

Next, we analyze the ground state energy for different values of W . In Fig. 5, we present the real and imaginary components of the persistent current alongside their corresponding ground state energies. Both the real and imaginary parts of the ground state energy exhibit continuous variation with flux, except at a few exceptional points. For $W = 0.5$, we observe a steeper change in the slope in both real and imaginary cases, leading to a higher PC compared to lower W . However, as W increases further, the spectrum becomes increasingly flattened in both components, ultimately resulting in a diminished PC.

C. Interplay of Disorder and Non-Hermiticity

To further investigate the impact of the complex phase of AAH modulation (h), we plot the maximum persistent current as a function of h in Fig. 6. The left panel represents the maximum of the real part of the current, while the right panel illustrates the maximum of the imaginary part. From this figure, we observe that within a certain range of h , the persistent current increases, indicating an enhancement in transport properties. However, at higher values of h , the current begins to decline again, suggesting a non-monotonic dependence of persistent current on the complex phase. Similarly, to investigate the impact of AAH modulation strength, we plot the maximum PC as a function of W in Fig. 7. Interestingly, we observe an unconventional behavior—the persistent current initially increases with disorder strength but starts to decline at higher values of W . This non-trivial trend implies that moderate disorder can increase transport while excessive disorder suppresses it.

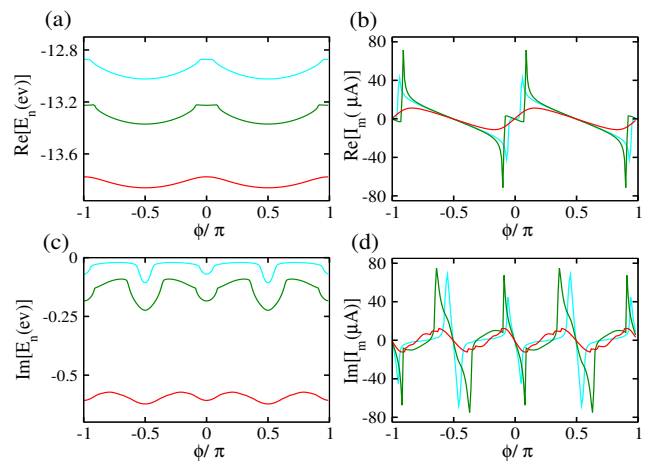


FIG. 5. (Color online). Real and imaginary parts of the ground state energy versus AB flux ((a) and (c)) and real and imaginary parts of maximum PC versus AB flux ((b) and (d)) where cyan, orange and green curves represents the results for $W = 0.25, 0.5$ and 0.75 respectively.

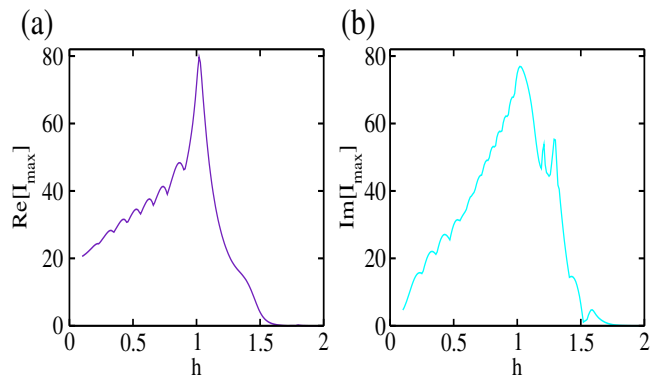


FIG. 6. (Color online). Real and imaginary components of maximum current as a function of h where W fixed at 0.5 .

We provide a density plot that maps the relationship between W , h , and the current; to determine the optimal values of them that maximize the PC. This visualization allows us to identify the specific regions in parameter space where the persistent current reaches its peak, providing deeper insight into the interplay between AAH modulation strength and complex phase in governing the system's transport properties. Fig. 8 indicates that the maximum persistent current occurs in the regime where the disorder strength, W is relatively small, while the complex phase, h is relatively higher. This suggests that moderate non-Hermiticity can enhance transport, whereas, as expected, excessive disorder suppresses it, highlighting the intricate interplay between quasiperiodic modulation and non-Hermiticity in determining the system's conductive properties.

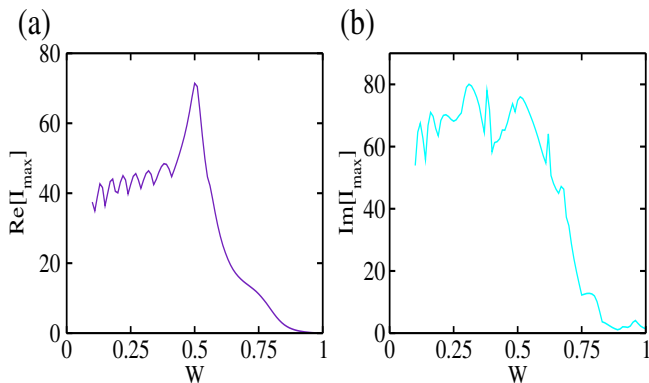


FIG. 7. (Color online). Response of real and imaginary components of maximum PC with disorder strength W , where h fixed at 1.

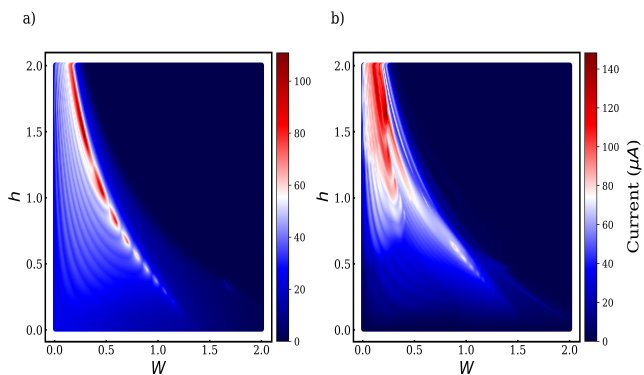


FIG. 8. (Color online). Variation of real and imaginary parts of maximum PC with h and W .

D. Interacting case

We investigate whether the observed trends in the non-interacting case hold in the presence of local many-body effects. We consider a finite size ring (12 sites ring to be specific) described by the Hubbard Hamiltonian with non Hermitian AAH term. We apply an exact diagonalization routine to the matrix, obtaining both the real and imaginary eigenvalues along with their corresponding eigenvectors.

In Fig. 9, we present the real part of the persistent current on the left and the imaginary part on the right varying disorder strengths. In the interacting case, we observe a slight enhancement in the real part of the PC, while the imaginary part experiences a more significant increase within certain flux windows. Although interactions compete with disorder to some extent, the overall trends remain consistent with those observed in the non-interacting case, indicating that the fundamental effects of non-hermiticity and quasiperiodic modulation persist even in the presence of electron interactions.

The observed trend holds true when the interaction strength in the system is relatively small. However, in a strongly interacting system, this enhancement effect disappears. Fig. 10 shows that the maximum of both the

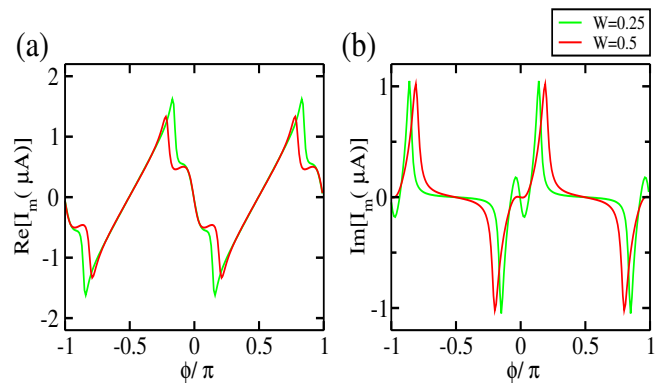


FIG. 9. (Color online). Persistent current of disordered ring I as a function of ϕ in the presence of onsite Hubbard interaction. (a) Real and (b) imaginary I for $U = 1.5$.

real and imaginary parts of the PC increases for smaller U values but significantly diminishes at higher U . This suggests that while weak interactions may still allow for enhancement effects, similar to the non-interacting case, strong interactions suppress the persistent current, possibly due to increased localization and reduced charge mobility. The main point is that by considering both the non-interacting and interacting systems, we have found a huge interplay between the disorder and non-Hermiticity in terms of generating persistent current in the system, where the moderate disorder maximizes the PC and we have established the microscopic reasons for it.

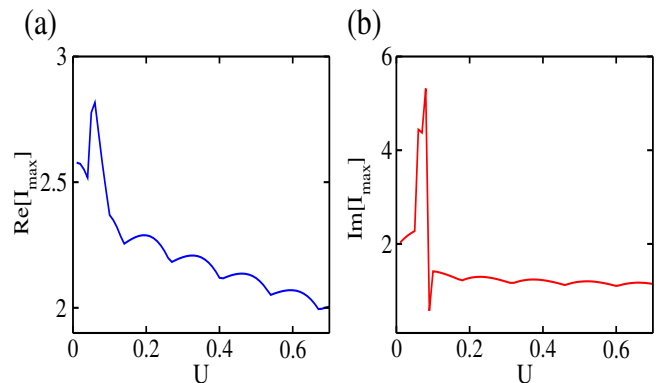


FIG. 10. (Color online). Max $[I]$ as a function of on-site Hubbard interaction. (a) Real and (b) imaginary currents. The half-filled system consists of $N = 12$ sites.

IV. SUMMARY AND OUTLOOK

In summary, this study has explored the impact of disorder and non-Hermiticity on the persistent current in a mesoscopic ring subjected to an AB flux. The disorder and non-Hermiticity have been introduced via the AAH model, with the latter arising from the phase of the onsite AAH modulation. The system has been described using a TB Hamiltonian, and the ground state energy

has been obtained through diagonalization. By differentiating the ground state energy with respect to the AB flux, we have computed the persistent current and have observed both its real and imaginary components due to non-Hermiticity. We have thoroughly analyzed the influence of various system parameters on these components of PCs, considering both non-interacting and interacting scenarios. In the interacting case, we have incorporated spin degrees of freedom and included repulsive on-site Hubbard interaction. All calculations have been performed for a half-filled system. The key findings of our study have been as follows.

- The interplay between disorder strength (W) and non-Hermiticity (h) is very promising. For non-zero disorder strength, both the real and imaginary parts of the PC increases with h and reaches its maximum value at sufficiently high value of h .
- The systematic study of the interplay between the AAH strength and non-Hermiticity reveals that, in presence of h , an enhancement of PC occurs with disorder strength and it increases till a critical value of w .
- The simultaneous variation of w and h indicates that the enhancement of PC takes place for a wide range of parameter values.
- Numerical simulations indicate a behavior similar

to the non-interacting case for moderate interaction strength, suggesting that the interaction effect does not significantly alter the characteristics of PC.

- Furthermore, we find a similar enhancement of PC with interaction both in real and imaginary counterpart in presence of disorder as present in its Hermitian analogue.

• Notably, this enhancement in PC has been attained without relying on any hopping dimerization mechanism which proves that our results are applicable to any non-Hermitian quasiperiodic ring without imposing any constraints in the system.

Our results highlight a potential regime where non-Hermitian quasiperiodicity and electron correlations can work synergistically to enhance persistent currents, offering new insights in the future research of non-Hermitian quasiperiodic systems.

ACKNOWLEDGMENTS

SS is thankful to DST-SERB, India (File number: PDF/2023/000319) for providing her research fellowship. SKP acknowledges the JC Bose fellowship and SERB, Govt. of India for the financial assistance.

-
- [1] M. Büttiker, Y. Imry, and R. Landauer, Phys. Lett. A **96**, 365 (1983).
- [2] I. O. Kulik, JETP Lett. **11**, 275 (1970).
- [3] L. P. Lévy, G. Dolan, J. Dunsmuir, and H. Bouchiat, Phys. Rev. Lett. **64**, 2074 (1990).
- [4] H. F. Cheung, and Y. Gefen, and E. K. Riedel, and W. H. Shih, Phys. Rev. B **37**, 6050 (1988).
- [5] V. Ambegaokar and U. Eckern, Phys. Rev. Lett. **65**, 381 (1990).
- [6] B. L. Altshuler, Y. Gefen, and Y. Imry, Phys. Rev. Lett. **66**, 88 (1991).
- [7] G. J. Jin, Z. D. Wang, A. Hu, S. S. Jiang, Phys. Rev. B **55**, 9302 (1997).
- [8] S. K. Maiti, J. Chowdhury, and S. N. Karmakar, J. Phys.: Condens. Matter **18**, 5349 (2006).
- [9] J. S. Sheng, and K. Chang, Phys. Rev. B **74**, 235315 (2006).
- [10] E. M. Q. Jariwala, P. Mohanty, M. B. Ketchen, and R. A. Webb, Phys. Rev. Lett. **86**, 1594 (2001).
- [11] R. Deblock, R. Bel, B. Reulet, H. Bouchiat, and D. Mailly, Phys. Rev. Lett. **89**, 206803 (2002).
- [12] H. Bluhm, N. C. Koshnick, J. A. Bert, M. E. Huber, and K. A. Moler, Phys. Rev. Lett. **102**, 136802 (2009).
- [13] A. C. Bleszynski-Jayich, W. E. Shanks, B. Peaudecerf, E. Ginossar, F. von Oppen, L. Glazman and J. G. E. Harris, Science **326**, 272 (2009).
- [14] X. Chen, Z-Y, Deng, W. Lu, and S. C. Shen, Phys. Rev. B **61**, 2008 (2000).
- [15] M. Abraham and R. Berkovits, Phys. Rev. Lett. **70**, 1509 (1993).
- [16] F.V. Kusmartsev, Phys. Lett. A **251**, 143 (1999).
- [17] Z-G, Chen, L. Wang, G. Zhang, and G. Ma, Phys. Rev. Appl. **14**, 024023 (2020).
- [18] T. Liu and H. Guo, Phys. Lett. A **382**, 024023 (3287).
- [19] S. Aubry and G. André, Ann. Isr. Phys. Soc. **3**, 133 (1980).
- [20] P. G. Harper, Proc. R. Soc. London, Ser. A **68**, 874 (1955).
- [21] M. Rossignolo and L. Dell'Anna, Phys. Rev. B **99**, 054211 (2019).
- [22] S. Sil, S. K. Maiti, and A. Chakrabarti, Phys. Rev. Lett. **101**, 076803 (2008).
- [23] S. Roy, S. Ganguly, and S. K. Maiti, Sci. Rep. **13**, 4093 (2023).
- [24] T. Eichelkraut, R. Heilmann, S. Weimann, S. Stützer, F. Dreisow, D. N. Christodoulides, S. Nolte, and A. Szameit, Nat. Commun. **4**, 2533 (2013).
- [25] X. Luo, T. Ohtsuki, and R. Shindou, Phys. Rev. Lett. **126**, 090402 (2021).
- [26] K. Kawabata and S. Ryu, Phys. Rev. Lett. **126**, 166801 (2021).
- [27] L. G. Celardo, M. Angeli, F. Mattiotti, and R. Kaiser, EPL **145**, 35002 (2024).
- [28] X. Xia, K. Huang, S. Wang, and X. Li, Phys. Rev. B **105**, 014207 (2022).
- [29] A. Padhan, S. R. Padhi, and T. Mishra, Phys. Rev. B **109**, L020203 (2024).
- [30] C. M. Bender, and S. Boettcher, Phys. Rev. Lett. **80**, 5243 (1998).
- [31] C. M. Bender, Rep. Prog. Phys. **70**, 947 (2007).
- [32] R. E-Ganainy, K. G. Makris, M. Khajavikhan, Z. H. Muslimani, S. Rotter, and D. N. Christodoulides, Nat. Phys. **14**, 11 (2018).
- [33] Q. Li, J.-J. Liu, and Y.-T. Zhang, Phys. Rev. B **103**, 035415 (2021).
- [34] S. Ganguly and S. K. Maiti, arXiv:2412.14593 (2024).
- [35] S. Roy and S. K. Maiti, arXiv:2501.06447 (2025).
- [36] E. Gambetti, Phys. Rev. B **72**, 165338 (2005).

- [37] O. I. Pâțu1 and D. V. Averin, Phys. Rev. Lett. **128**, 096801 (2022).
- [38] S. R. White, Phys. Rev. Lett. **69** 2863 (1992).
- [39] U. Schollwöck, Ann. Phys. **326** 96 (2011).